Vladan Nedelkovski, Milan Radovanović, Slađana Alagić*

Technical faculty in Bor, University of Belgrade, Bor, Serbia

Photocatalytic degradation of naphthalene, using various nanocomposite materials mostly based on metal oxides

ABSTRACT

Polycyclic aromatic hydrocarbons (PAHs) cause significant environmental and health concerns, necessitating effective remediation strategies. Specifically, biological treatments are only effective for PAH compounds with lower molecular weights, while for the efficient elimination of more complex PAH structures, the photocatalytic method is more recommended. Photocatalytic degradation has primarily relied on TiO₂-based materials. However, this review focuses on the utilization of various nanomaterials for the degradation or total removal of naphthalene from the environment, and especially from wastewater. Precisely speaking, the photocatalytic activity of various nanocomposite materials containing (predominately) metal oxides is discussed, with an emphasis on photocatalytic degradation mechanisms and the identification of degradation intermediates. Key findings reveal that these materials hold substantial promise, and that photogenerated holes, superoxide radicals, and hydroxyl radicals play crucial roles in the degradation processes, highlighting additionally the unique mechanisms of these processes. Important information about the intermediates and pathways of naphthalene photodegradation discussed in the mechanisms of degradation has been confirmed using gas chromatography-mass spectrometry (GC-MS).
Key words: Degradation mechanisms, naphthalene, nanomaterials, photocatalysis

1. INTRODUCTION

Polycyclic Aromatic Hydrocarbons (PAHs), a group of organic compounds characterized by multiple interconnected aromatic rings, are classified as persistent organic pollutants, primarily originating from processes such as incomplete fossil fuel combustions. They can be found in various other sources, including volcanic eruptions, forest fires, waste incineration, asphalt production, oil refining facilities, and aluminum production [1-3]. This class of compounds, along with the methods and procedures for their removal, has garnered considerable attention of researchers, especially regarding their substantial toxicity, mutagenicity, and carcinogenicity. The increasing presence of these hazardous micropollutants in aquatic environments, soils, sediments, and food has raised researchers' concerns significantly [4, 5].

*Corresponding author: Slađana Alagić

e-mail: salagic@tfbor.bg.ac.rs

Due to their low molecular weight (LMW) and low vapor pressure, PAHs with two (naphthalene, Nap) or three benzene rings (anthracene, phenanthrene), are considered extremely toxic but not generally carcinogenic to most exposed organisms. In contrast, PAHs with four or more rings (high molecular weight PAHs, HMW PAHs), are less volatile compounds, less available to the organisms, exhibiting in that way a lower toxicity but generally, a bigger carcinogenicity. The distribution of these substances in the environment can vary significantly, also depending on their volatility and consequently - mobility [6]. The United States Environmental Protection Agency (US EPA) has designated this group of compounds as priority pollutants. Sixteen priority PAHs are Nap, acenaphthene, acenaphthylene, anthracene, fluoranthene, fluorene, phenanthrene, pyrene, benzo[a]anthracene, chrysene, benzo[b]fluoranthene, benzo[k]fluoranthene, benzo[ghi]perylene, benzo[a]pyrene, dibenzo(a,h)anthracene, and indeno (1,2,3-cd)pyrene [1, 7-10]. As mentioned previously, the simplest PAH compound is Nap, consisting of two benzene rings, with a molar mass of 128.19 g/mol, solubility of 31.69 µg/L, and the vapor pressure of

0.087 mm Hg [1,9]. As such, Nap is the most volatile and the most (water) soluble PAH compound so it was found as the most present in waters, and especially in waste waters. Its concentrations vary depending on the location, i.e. on the closeness of the source of pollution. In clean rivers and lakes, the amount is usually less than 5 ng/L. However, it can be a bit higher in other places, reaching up to a few µg/L. In ground water that's not polluted, Nap is found at levels up to 0.03 µg/L. The sea waters have a maximum recorded amount of 300 ng/L. Rain water and tap water can have Nap at the level of 370 ng/L. However, in waters where the environment is highly polluted, Nap levels can be as high as 15.3 mg/L [11].

Given that these concentrations may represent a serious threat for aquatic organisms, and also, for humans (through the food chains) [7], various strategies have been investigated for the efficient elimination of Nap or other PAHs from liquids, as well as from other mediums. Within the realm of biological treatments, techniques such as bioremediation (including phytoremediation), have emerged as prevalent approaches for the removal of PAHs. These approaches exhibit suboptimal efficiency, require multiple days for PAH degradation, and entail labor-intensive procedures along with the unavailability of requisite for biological catalysts [12]. On the other hand, among physical-chemical treatment methodologies, the most frequently employed methods encompass membrane filtration, adsorption, advanced oxidation processes, and chemical precipitation [13].

In recent years, various groups of researchers have paid special attention to the relatively new method such as photodegradation of PAHs. This included the selection of catalytically active materials, identification of intermediate compounds and final products (practically, H_2O, and CO_2) with the determination of degradation mechanisms and the optimization of the photocatalytic degradation process [14-16].

Within the broad realm of processes of the photocatalytic degradation of organic pollutants, which are also known as Advanced Oxidation Processes (AOP), the characteristic mechanisms involve the initial formation of highly reactive •OH radicals. The electron (e^-) - hole (h^+) pairs also form as charge carriers in the metal nanoparticles; in practice, the e^- receives an additional portion of energy through the interaction with electromagnetic radiation from the ultraviolet/visible part of the energy spectrum; this energy is necessary for e^- removing from the valence (VB) to the conduction band (CB) [17,18]. According to this transfer, a formed h^+ represents a quasiparticle indicating the absence of an e^- in the atom (or crystal lattice). In such circumstances, the negative charge of e^- is balanced by the positive charge of the atomic nuclei, leaving a net positive charge at the location of the h^+. Holes in a metal or semiconductor crystal lattice can move through the lattice (similar to the e^-) and act as positively charged particles [19]. The recombination of these charge carriers (e^-, and h^+) signifies the annihilation of pairs, effectively ending their existence through mutual merging [20].
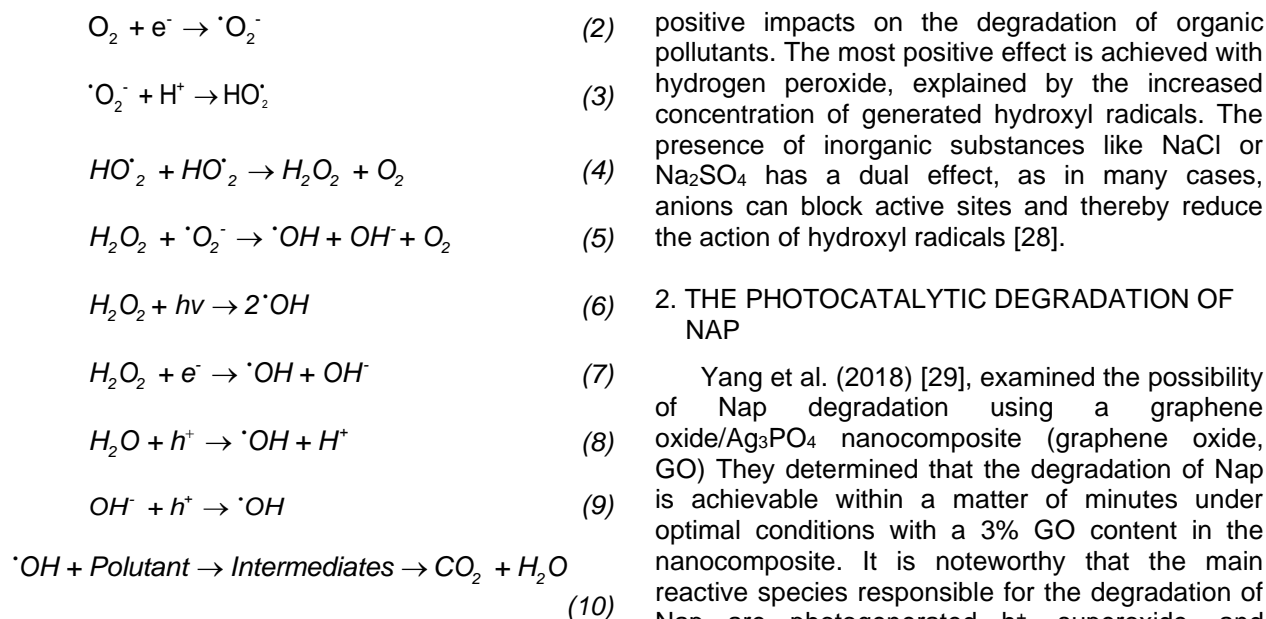
It is well known that the photocatalytic mechanisms are the most affected by the e^- pathway, which is influenced by the CB and VB of the catalysts. The energy of band structure, along with nano-structured bulk and surface properties, are crucial for photocatalytic reactions [21]. The size of the band gap determines the energy (of light) required to excite an e^- from the VB to the CB. A smaller band gap can absorb longer wavelengths of light (visible light), making the material active under solar light (which is desirable for photocatalysis) [22, 23].

When nanoparticles absorb an amount of energy equal to or greater than the energy of the energy gap or bandgap, a transition of e^- occurs, leading to their photoexcitation from the filled VB to the empty CB. Simultaneously, the induction of h^+ starts in the VB. When photo-induced charge carriers (e^- and h^+) are located at or near the material's surface (nanoparticles), due to the increasingly pronounced redox properties, two additional processes can take place. In the first process, e^- from the CB can participate in the formation of superoxide radicals ($^•O_2^-$) by reducing oxygen and further forming peroxides, which contribute significantly to the degradation of organic pollutants. In the second process, positively charged h^+ can oxidize water molecules or the OH^- group to $^•OH$ radicals, achieving the complete mineralization of organic pollutants [24, 25].

In aqueous solutions, the mechanism can proceed in five steps [26,27]: 1) Diffusion of pollutant molecules from the aqueous phase to the surface of nanomaterial; 2) Adsorption of pollutant molecules on the surface of nanoparticles (NPs); 3) Redox processes within the layer of adsorbed molecules; 4) Desorption of products and 5) Transport of product molecules into the aqueous phase.

For example, the entire mechanism of photocatalysis, occurring in the presence of zinc oxide nanoparticles (ZnO NPs), Abdullah et al. (2022) [26] presented through the reactions 1-10:

$$ZnO + hv \rightarrow e^- + h^+ \qquad (1)$$

$$O_2 + e^- \rightarrow {}^{\cdot}O_2^- \qquad (2)$$

$${}^{\cdot}O_2^- + H^+ \rightarrow HO_2^{\cdot} \qquad (3)$$

$$HO_2^{\cdot} + HO_2^{\cdot} \rightarrow H_2O_2 + O_2 \qquad (4)$$

$$H_2O_2 + {}^{\cdot}O_2^- \rightarrow {}^{\cdot}OH + OH^- + O_2 \qquad (5)$$

$$H_2O_2 + h\nu \rightarrow 2\,{}^{\cdot}OH \qquad (6)$$

$$H_2O_2 + e^- \rightarrow {}^{\cdot}OH + OH^- \qquad (7)$$

$$H_2O + h^+ \rightarrow {}^{\cdot}OH + H^+ \qquad (8)$$

$$OH^- + h^+ \rightarrow {}^{\cdot}OH \qquad (9)$$

$${}^{\cdot}OH + Polutant \rightarrow Intermediates \rightarrow CO_2 + H_2O \qquad (10)$$

h - Planck's constant, with a value of 6.62×10^{-34} J·s

υ - frequency of electromagnetic radiation

It is essential to note that the efficiency of photocatalysis is also influenced by the presence of many other factors such as, different formed chemical species; for example, other oxidizing agents - $(NH_4)_2S_2O_8$, $KBrO_3$, and H_2O_2, having positive impacts on the degradation of organic pollutants. The most positive effect is achieved with hydrogen peroxide, explained by the increased concentration of generated hydroxyl radicals. The presence of inorganic substances like NaCl or Na_2SO_4 has a dual effect, as in many cases, anions can block active sites and thereby reduce the action of hydroxyl radicals [28].

2. THE PHOTOCATALYTIC DEGRADATION OF NAP

Yang et al. (2018) [29], examined the possibility of Nap degradation using a graphene oxide/Ag_3PO_4 nanocomposite (graphene oxide, GO) They determined that the degradation of Nap is achievable within a matter of minutes under optimal conditions with a 3% GO content in the nanocomposite. It is noteworthy that the main reactive species responsible for the degradation of Nap are photogenerated h^+, superoxide, and hydroxyl radicals. It is well-known that, even without photodegradation, Nap undergoes moderate degradation due to its volatility. The degradation products of Nap in photodegradation were identified using gas chromatography-mass spectrometry (GC-MS). Based on the results, the researchers proposed two degradation pathways within the mechanisms illustrated in Fig. 1.
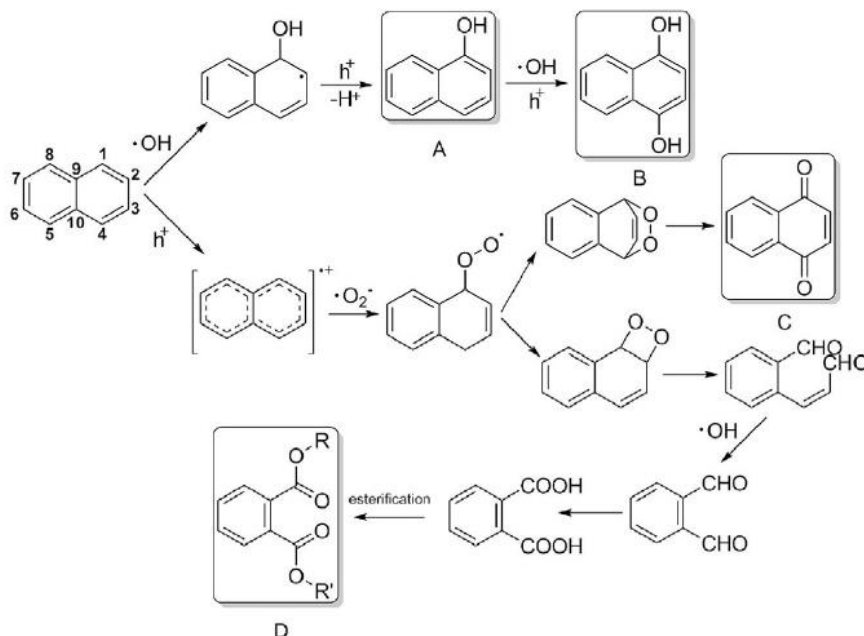

Figure 1. Potential pathways for the formation of primary intermediates in the photodegradation of Nap in the presence of GO/Ag_3PO_4 [29]

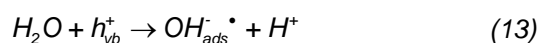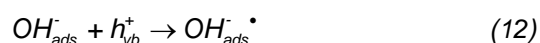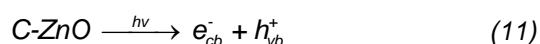According to the first reaction pathway, hydroxyl radicals can directly attack the position 1 of the Nap molecule, thus facilitating the formation of hydroxyl derivatives, namely 1-naphthol (A) or 1,4-dinaphthol (B). In the second reaction pathway, the primary degradation products of naphthalene are 1,4-naphtoquinone (C) and the dialkyl ester of

1,2-benzenedicarboxylic acid (D). Researchers did not conducted the identification of the further intermediates, but they stated that further degradation normally leads to the complete mineralization with the ultimate products being CO_2 and H_2O [29].
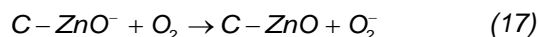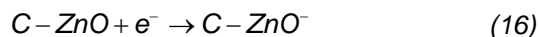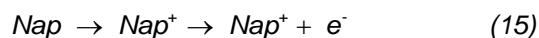
Xue et al. (2018) [30], achieved the complete photocatalytic degradation of Nap (along to the CO_2, and H_2O) on carbon-doped ZnO nanoparticles. The deposition of so-called "C dots", known as the doping of C atoms, positively affects the catalytic activity of ZnO crystals (C-ZnO), resulting in faster degradation of PAHs, as confirmed by the results of the photocatalytic degradation of Nap. The enhanced photocatalytic activity of the C-ZnO nanocatalyst compared to pure ZnO can be explained by the fact that photo-generated e^- plays a crucial role in the degradation of PAHs. In the photocatalytic process, C-ZnO generates more e^- and h^+ by absorbing sustainable energy to enhance photocatalytic activity. On the surface of C-ZnO, holes oxidize OH^- and H_2O to form $OH^- \cdot$ species. Simultaneously, electrons react with adsorbed O_2 molecules to generate superoxide radicals [30].

In the experiment of Xue et al. (2018) [30], an optimal quantity of a nanocatalyst in the form of a solid solution, C-ZnO SS, 50 mg was added to a 50 mL mixture of Nap and anthracene (in concentrations of 20 mg/L each). Subsequently, the catalytically active material was mixed with the prepared synthetic solution in the dark, which is a common step in photocatalytic degradation to adsorb the molecules of a specific compound on the surface of nanoparticles (i.e., to reach adsorption-desorption equilibrium). After 5 hours of irradiation (ultraviolet, UV, lamp, 8 W, λ = 365 nm, 0.92 mW/cm^2), it was determined that Nap was completely removed from the solution. The researchers noticed that Nap, when exposed to UV radiation alone, did not exhibit signs of self-degradation.

Xue et al. (2018) [30] concluded that in the case of Nap molecules (in their excited state), an e^- transfer occurs to the conduction band of C-ZnO, resulting in the transformation of O_2 molecules into superoxide radicals:

$$C\text{-}ZnO \xrightarrow{\ h\nu\ } e^-_{cb} + h^+_{vb} \qquad (11)$$

$$OH^-_{ads} + h^+_{vb} \rightarrow OH^{-\bullet}_{ads} \qquad (12)$$

$$H_2O + h^+_{vb} \rightarrow OH^{\bullet}_{ads} + H^+ \qquad (13)$$

$$O_2 + e^-_{cb} \rightarrow O^{\bullet}_2 \qquad (14)$$

At the same time, the molecules of Nap (in the excited state) transfer e^- into the conduction band of C-ZnO SS, where the capturing of O_2 occurs as well as the formation of O_2^- (formulas: 15-16) [30]:

$$Nap \rightarrow Nap^+ \rightarrow Nap^+ + e^- \qquad (15)$$

$$C - ZnO + e^- \rightarrow C - ZnO^- \qquad (16)$$

$$C - ZnO^- + O_2 \rightarrow C - ZnO + O_2^- \qquad (17)$$

Furthermore, within the C-ZnO structure, the possibility of recombination of charge carriers is reduced, resulting in a shorter Nap degradation time, i.e., in complete mineralization to final products - CO_2 and H_2O [30].

Mukwevho and colleagues (2020) [8] investigated the efficiency of Nap adsorption in the presence of ZnO nanoparticles, as well as binary ZnO/Ag and ternary ZnO/Ag/GO nanocomposites, concerning the concentration of residual Nap in the solution relative to the contact time between the adsorbent and adsorbate. It was observed that the adsorption of Nap molecules on all investigated nanocatalysts occurs relatively rapidly, with over 40% of Nap molecules adsorbed within 1 min of exposure to the adsorbent surface in a synthetic aqueous solution. ZnO and ZnO/Ag nanocatalysts achieved a slightly higher adsorption efficiency, with approximately 65% of Nap being adsorbed within 5 min reaching adsorption-desorption equilibrium. However, within 20 min after interaction with the surface of the ZnO/Ag/GO nanocomposite material, the adsorption of Nap reached approximately 80%. The continuous increase in the adsorption efficiency of ZnO/Ag/GO over time can be attributed to the larger active surface area due to the presence of GO material. In addition, the GO framework in the ZnO/Ag/GO nanocomposite is enriched with p-electrons, which enhances p-p interactions with the aromatic rings of Nap and facilitates the adsorption process [8].

Farhadian et al. (2016) [31], concluded in their experiment (under visible light and using a nanocomposite of WO$_3$-MWCNT, multi-wall carbon nanotubes), that Dewar's reactivity (number "Nu", which reflects the localization energy in the aromatic benzene rings), is lower for position 1 (1.81) than for position 2 (2.12) (Fig. 2). This implies that position 1 is more susceptible to the attack by reactive hydroxyl or superoxide species.

The main product/intermediate in the early stages of Nap degradation is considered to be 1-naphthalenol (II). This intermediate is formed by the attack of hydroxyl radicals on position 1 of the Nap molecule. Additionally, when superoxide radicals attack the position 2 of Nap molecule, hydroperoxyl radicals are released, and 1-

naphthalenol is formed. Consequently, this process repeats, leading to the further formation of 1,4-naphthalenediol (III). Further, the attack of OH$^•$ radicals on the position 2 of the 1,4-naphthalenediol (III) molecule leads to the release of a water molecule, while the attack of superoxide radicals on the position 4 eventually releases hydroperoxyl radicals, which results in the

formation of 1,4-naphthalene ketone (IV). There is also an alternative reaction pathway in which superoxide radicals attack the position 1 of Nap. In this pathway, 1,2-benzenedicarboxylic acid (VI) is formed, and acetylene (C_2H_2) is released, causing the opening of one aromatic ring. The researchers concluded that species such as OH$^•$ and $O_2^{•−}$ are responsible for Nap degradation [31].
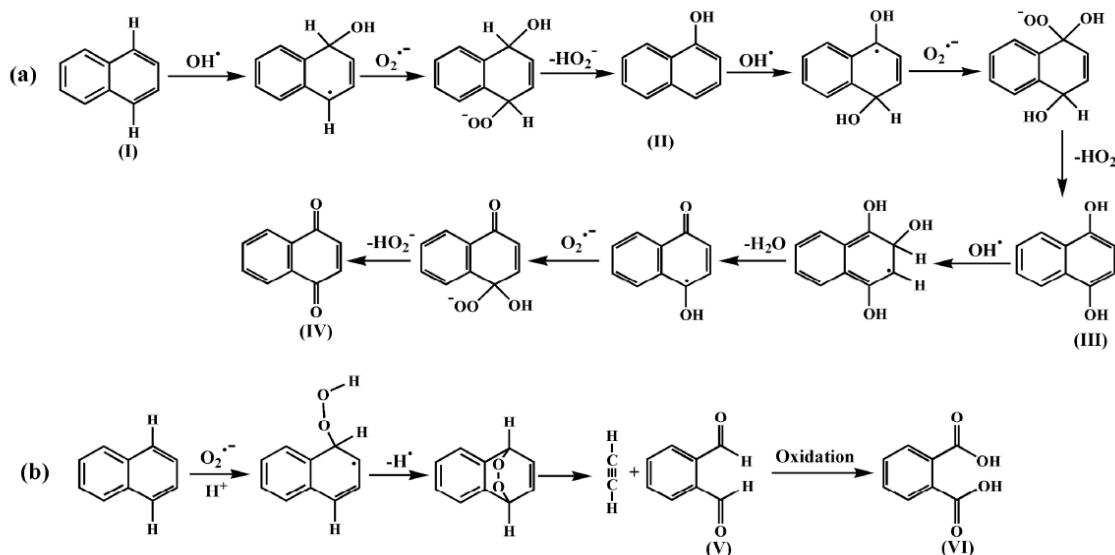

Figure 2. Proposed mechanism for Nap degradation in the presence of WO$_3$-MWCNT nanocomposites under visible light; the presence of intermediates labeled as (III) and (V) was not confirmed in the study [31]

Further, in the experiment of Farhadian et al. (2016) [31], the comparison of photocatalytic activity of WO$_3$ nanocrystals with WO$_3$-MWCNT nanocomposite showed that the efficiency of Nap photodegradation was negligible when using pure WO$_3$ nanocrystals. However, the combination of WO$_3$ and MWCNT materials resulted in a significantly improved photocatalytic activity under visible light. A 570 W xenon lamp was used as the light source, and a UV filter "L41" was employed to eliminate UV light ($\lambda < 400$ nm). In their research, GC/MS analysis of the sample after 4 hours of reaction revealed a series of peaks with different retention times (Rt) ranging from 5 to 25 min. The results indicated moderate degradation of Nap into 1-naphthalenol in the presence of WO$_3$ and under visible light. However, when degrading Nap in the presence of WO$_3$-MWCNT, three intermediate products were detected at Rt values of 9.9, 13.15, and 14.4 min. According to the obtained mass spectra, the peaks recorded at Rt values of 9.9, 13.15, 14.4, and 18.27 min were attributed to Nap, 1,4-naphthalenedione, 1-naphthalenol, and 1,2-benzenedicarboxylic acid, respectively (with 1-naphthalenol being the predominant product). Researchers concluded that the intermediate products identified in the photocatalytic degradation

of Nap can significantly depend on the light source and the type of photocatalytically active material.

Zhang et al. (2019) [32] proposed a mechanism for Nap degradation under light in the wavelength range of 400-780 nm, in the presence of Fe$_3$O$_4$ nanoparticles, with and without hydrogen peroxide. The suggested degradation mechanism can be found in Fig. 3.

Firstly, as shown in Fig. 3, the photocatalytic degradation of Nap using Fe$_3$O$_4$ was conducted without the presence of H$_2$O$_2$, resulting in the primary products of 1,2-diphenylbutadiene (1) or 1,4-diphenylbutadiene (2), 1,3-diphenylpropane (3), and 1,2-diphenylcyclopropane (4). This suggests that the degradation process primarily occurs through the opening of the aromatic ring in Nap molecules and continuous catalytic alkylation, degradation, and rearrangement between open-ring products to form diphenyl structures. When Fe$_3$O$_4$ is exposed to radiation, both: holes and electrons are generated on its surface. Fe(III) is reduced to Fe(II) after receiving an electron, and the oxidation process can proceed via the transfer of one electron, resulting in the formation of a cationic Nap radical. Strong adsorption of Nap on the surface of Fe$_3$O$_4$ facilitates electron transfer from the excited Fe(III)-Fe$_3$O$_4$ to organic molecules, initiating the photodegradation of Nap [32].
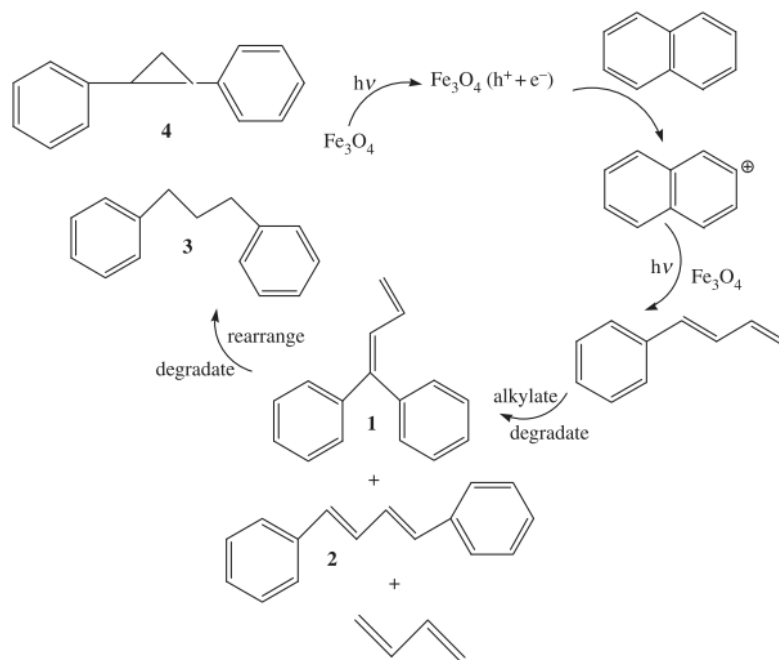
Figure 3. Proposed mechanism for Nap degradation in the presence of Fe_3O_4 and the absence of hydrogen peroxide [32]

In the first step, the opening of the adsorbed Nap cation's aromatic ring appears to form phenylbutadiene under visible light radiation. Subsequently, phenylbutadiene undergoes alkylation with another phenylbutadiene molecule, followed by Lewis acid-catalyzed degradation on the catalyst's surface to generate products 1, 2, and butadiene. Products 1 and 2 further undergo continuous degradation and/or rearrangement to form intermediates 3 and 4, catalyzed by Lewis acid on the catalyst's surface. In the presence of H_2O_2, temporary Fe(II) or Fe(III) in Fe_3O_4 can bind and reduce H_2O_2 to produce ·OOH and/or ·OH radicals with high redox potential. Therefore, it is concluded that the degradation process occurs through photocatalysis and the oxidative action of ·OOH and/or ·OH radicals.
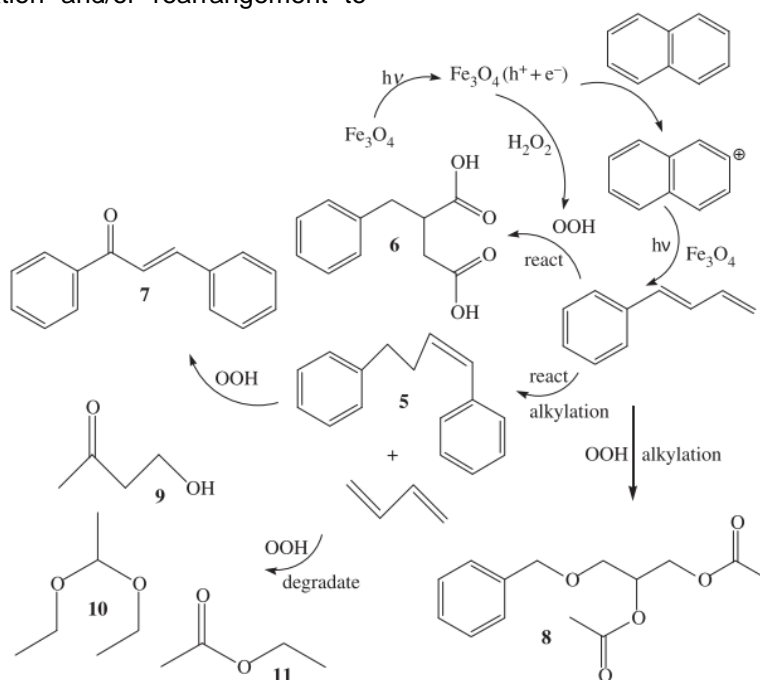

Figure 4. Proposed mechanism of Nap degradation in the presence of Fe_3O_4 and hydrogen peroxide [32]

As a result, Nap photocatalytic degradation and oxidation occur simultaneously in the presence of H_2O_2. Consequently, the degradation products differ significantly compared to the previous case due to the oxidative effect. Based on the obtained GC-MS spectra analysis, a reaction mechanism has also been proposed, as shown in Fig. 4.

The primary products identified through GC-MS analysis include 1,4-diphenyl butene-1 (5), benzyl succinic acid (6), 1,3-diphenyl acryl ketone (7), (benzyl methyl ether)-ethyl diacetate (8), and hydroxy-ethyl methyl ketone (9). Additionally, the reaction mixture contains a small amount of 2-ethoxy-ethyl ether (10) and ethyl acetate (11), as depicted in Fig. 4. The formation of these products in the presence of H_2O_2 reveals that the photocatalytic degradation, in this case, commences with the opening of the aromatic ring, followed by oxidation, alkylation, and the decomposition of newly formed products with an open ring [32].

Some researchers however did not discuss or present possible photocatalytic degradation mechanism pathways. For example, Khatibi et al. (2021) [33] determined that reducing of the concentration of pollutants enhances the efficiency of their removal. Specifically, they observed that a 100 ppm concentration of Nap was removed with an efficiency of 93,8% using ZnO nanoparticles within 60 minutes at a pH of 0.8. Researchers stated that the swift breakdown of Nap molecules within the initial 10 min of the procedure is primarily due to the generation of free radicals, a result of e^- excitation in nanoparticles. While the activation of zinc oxide nanoparticles and the creation of hydroxyl free radicals remained consistent over the extended contact period, the presence of intermediate organic compounds, formed through the Nap degradation process, led to the utilization of some hydroxyl radicals in breaking down these compounds. Consequently, this led to a diminished efficiency in the removal of Nap.

In a separate study, Sekar et al. (2018) [34], successfully produced Fe-doped ZnO nano-particles embedded in polyvinyl alcohol (PVA) nanofibers, with the PVA concentration finely tuned to 8 wt% (nanofibers were extremely uniform and smooth). Their degradation experiments demonstrated 96% efficiency in degrading an initial Nap concentration of 40 ppm. The enhancement in this efficiency was attributed to the Fe doping of the photocatalyst, with doping leading to a narrowing of the band gap, the creation of impurity energy levels, and the formation of oxygen vacancies. These vacancies serve as e^- acceptors, trapping electrons, while interstitial oxygen plays a role as a "shallow trap" for holes. This dual action effectively prevents the recombination of photogenerated e^- and h^+, thus boosting the efficiency. Additionally, the nano-texturing achieved through the calcination of nanofibers significantly increases the surface-to-volume ratio, which in turn enhances photocatalytic activity. The calcination process also improves the surface morphology of the nanofibers.

3. CONCLUSION

Advanced oxidation processes are acknowledged for their non-destructive, cost-efficient, and exceptionally effective nature. This is not only due to their high efficiency in breaking down substances but also because they can minimize the creation of potentially harmful byproducts. This quality plays a critical role in maintaining the ecological balance and preventing further adverse effects on the environment; consequently, the present review study may be of importance for environmental preservation and mitigating detrimental environmental consequences.

Over recent years, several research groups have devoted particular attention to the degradation of PAHs through photodegradation. This involves: selecting catalyst materials with high activity, recognizing intermediates and final products, understanding degradation mechanisms, and fine-tuning the complete process of photocatalytic degradation. In the past two decades, the greatest attention has been paid on the use of zinc oxide and titanium oxide as primary metal oxide materials for improving the efficiency of degradation of different organic compounds. Table 1 summarizes the available data on the photocatalytic degradation of Nap.

Degradation pathways reveal that hydroxyl radicals usually directly attack position 1 of the Nap molecule, causing the opening of one aromatic ring. Usual intermediates are reported to be 1-naphthalenol, 1,4-naphthalene dione, and 1,2-benzene dicarboxylic acid (among the others), with 1-naphthalenol being the predominant product, while the final products are H_2O and CO_2.

Table 1. Summary table of the presented examples of photocatalytic degradation of Nap

Nanomaterial	Some important parameters of the experiment	Methods for the identification of degradation products	Degradation efficiency	Reference
ZnO	50 mg/L Nap; VIS (250 W); 25℃; 30 min	/	85%	[8]
ZnO/Ag			86%	
ZnO/Ag/GO			92%	
GO/Ag$_3$PO$_4$	600 µg/L Nap; 1 g/L GO/Ag$_3$PO$_4$; VIS (300 W); 7.5 min	GC-MS	82,1%	[29]
WO$_3$	10 ppm Nap; 50 mg WO$_3$ or WO$_3$/MWCNT; VIS (570 W); 25℃; 120 min	GC-MS	28%	[31]
WO$_3$/ MWCNT			100%	
ZnO	50 µg/L Nap; 10 mg Cu-ZnO/50 mL; VIS (500 W); 25℃; 120 min	/	10%	[35]
Cu-ZnO			17.5%	
Fe$_3$O$_4$	0.2 mmol of Nap dissolved in 100 mL ethanol + 100 mL deionized water; 0.3 g Fe$_3$O$_4$; VIS (300 W); 25℃; 8 hours	GC-MS	81.5% in the presence of H$_2$O$_2$; 74.3% in the absence of H$_2$O$_2$	[32]
ZnO	100 ppm Nap; 100 ppm ZnO; pH = 0.8; 60 min	GC-MS	93.8%	[33]
ZnO	40 ppm Nap; 30 mg Fe-ZnO/PVA/500 mL; UV (16 W); pH = 7; 37℃; 240 min	/	60%	[34]
Fe-ZnO			72%	
Uncalcined Fe-ZnO/PVA			81%	
Calcined Fe-ZnO/PVA			96%	
ZnO	20 mg/L Nap; 50 mg ZnO or C-ZnO; UV; 25℃; 5 hours	/	55%	[30]
C-ZnO SS			100%	

4. REFERENCES

[1] S.Č.Alagić, B.S. Maluckov, V.B.Radojičić (2015). How can plants manage polycyclic aromatic hydrocarbons? May these effects represent a useful tool for an effective soil remediation? A review, Clean Technologies and Environmental Policy, 17(3), 597-614.

[2] S.O. Baek, R. A. Field, M.E. Goldstone, P.W. Kirk, J.N.Lester, R. Perry (1991) A review of atmospheric polycyclic aromatic hydrocarbons: Sources, fate and behavior. Water, Air, and Soil Pollution, 60(3-4), 279–300.

[3] A.T.Lawal (2017) Polycyclic aromatic hydrocarbons. A review. Cogent Environmental Science, 3, 1–89.

[4] D.F.Kalf, T.Crommentuijn, E.J. Van de Plassche (1997) Environmental quality objectives for 10 polycyclic aromatic hydrocarbons (PAHS), Ecotoxicology and Environmental Safety, 36, 89–97.

[5] S.J.Varjani, R.R.Joshi, P.Senthil Kumar, V.K. Srivastava, V.Kumar, C.Banerjee, R.Praveen Kumar (2018) Polycyclic Aromatic Hydrocarbons from Petroleum Oil Industry Activities: Effect on Human Health and Their Biodegradation, Energy, Environment and Sustainability, 185–199.

[6] V.H. Nguyen, L.A. Phan Thi, Q. Van Le, P. Singh, P. Raizada, P. Kajitvichyanukul (2020) Tailored photocatalysts and revealed reaction pathways for photodegradation of polycyclic aromatic hydrocarbons (PAHs) in water, soil and other sources, Chemosphere, 260, 127529.

[7] S.Č. Alagić, V.P. Stankov Jovanović, V.D. Mitić, J.S. Cvetković, G.M. Petrović G.S. Stojanović (2016) Bioaccumulation of HMW PAHs in the roots of wild blackberry from the Bor region (Serbia): Phytoremediation and biomonitoring aspects, Science of The Total Environment, 562, 561-570.

[8] N.Mukwevho, R.Gusain, E.Fosso-Kankeu, N. Kumar, F.Waanders, S.S. Ray (2020) Removal of naphthalene from simulated wastewater through adsorption-photodegradation by ZnO/Ag/GO nanocomposite. Journal of Industrial and Engineering Chemistry, 81, 393-404.

[9] A.Papludis, A.Simonović, S.Alagić (2022) Sadržaj policikličnih aromatičnih ugljovodonika u zemljištu formiranih tokom spaljivanja e-otpada na mestima njegovog neadekvatnog odlaganja i reciklaže / The Content of Polycyclic Aromatic Hydrcarbons in Soil Formed During Incineration of E-waste at the Sites of its Inadeqate Disposal and Recycling. Zaštita materijala / Materials protection, 63(2), 165-176.

[10] Z. Zelinkova, T. Wenzl (2015) The Occurrence of 16 EPA PAHs in Food – A Review. Polycyclic Aromatic Compounds, 35, 248–284.

[11] ECB report (2003) European Chemicals Bureau, "Naphthalene, Summary Risk Assessment Report" Institute for Health and Consumer Protection, European Communities, 2003. (https://echa.europa.eu/documents/10162/e1dc4188-c5b1-444d-8ff1-71002ebe12d6)

[12] S.S.M.Hassan, W.I.Azab, H.R. Ali, M.S.Mansour (2015) Green synthesis and characterization of ZnO nanoparticles for photocatalytic degradation of anthracene, Advances in Natural Sciences: Nanoscience and Nanotechnology, 6, 045012.

[13] I.Gutierrez-Urbano, M.Villen-Guzman, R.Perez-Recuerda, J.M.Rodriguez-Maroto (2021) Removal of polycyclic aromatic hydrocarbons (PAHs) in conventional drinking water treatment processes, Journal of Contaminant Hydrology, 243, 103888.

[14] G.Eker, M.Hatipoglu (2019) Effect of UV wavelength, temperature and photocatalyst on the removal of PAHs from industrial soil with photodegradation applications, Environmental technology, 40, 3793–3803.

[15] G. Karaca, Y. Tasdemir (2014) Migration of PAHs in food industry sludge to the air during removal by UV and TiO_2. Science of The Total Environment, 488–489, 356–361.

[16] M.A.Sliem, A.Y.Salim, G.G.Mohamed (2019) Photocatalytic degradation of anthracene in aqueous dispersion of metal oxides nanoparticles: Effect of different parameters, Journal of Photochemistry and Photobiology A: Chemistry, 371, 327–335.

[17] A.L.Stanford, J.M.Tanner (1985) 23-Early Quantum Physics, Physics for Students of Science and Engineering, Academic Press Inc., Orlando, p 691-716.

[18] P.A. Tipler, R.A. Llewellyn (2008) Modern Physics (5ft ed.). W. H. Freeman and Company, New York, pp 124-125.

[19] N.W.Ashcroft, N.D.Mermin (1976) Solid State Physics (1st ed.). Holt, Rinehart, and Winston, New York, pp 299–302.

[20] V.K. Khanna (2005) Physical understanding and technological control of carrier lifetimes in semiconductor materials and devices: A critique of conceptual development, state of the art and applications, Progress in Quantum Electronics, 29(2), 59–163.

[21] D.Maarisetty, S.Mahanta, A.K.Sahoo, P. Mohapatra, S.S.Baral (2020) Steering the charge kinetics in dual-functional photocatalysis by surface dipole moments and band edge modulation: A defect study in TiO_2-rGO-ZnS composite, ACS Applied Materials & Interfaces, 12(10), 11679–11692.

[22] Y.R.Tang, Y.Zhang, J.X.Cao (2016) Modulating the band gap of a boron nitride bilayer with an external electric field for photocatalyst, Journal of Applied Physics, 119(19), 195303.

[23] S.S.M. Bhat, N.G. Sundaram (2013) Efficient visible light photocatalysis of Bi_4TaO_8Cl nanoparticles synthesized by solution combustion technique. RSC Advances, 3(34), 14371.

[24] E.Gaggero, P.Calza, E.Cerrato, M.C.Paganini (2021) Cerium-, europium- and erbium-modified ZnO and ZrO_2 for photocatalytic water treatment applications: A review. Catalysts, 11(12), 1059.

[25] E.Valadez-Renteria, J.Oliva, V.Rodriguez-Gonzalez (2022) Photocatalytic materials immobilized on recycled supports and their role in the degradation of water contaminants: A timely review, Science of The Total Environment, 807(2), 150820.

[26] F.H. Abdullah, N.H.H.A. Bakar, M.A. Bakar (2022) Current advancements on the fabrication, modification, and industrial application of zinc oxide as photocatalyst in the removal of organic and inorganic contaminants in aquatic systems, Journal of Hazardous Materials, 424(Part B), 127416.

[27] C.B.Ong, L.Y.Ng, A.W.Mohammad (2018) A review of ZnO nanoparticles as solar photocatalysts: Synthesis, mechanisms and applications, Renewable and Sustainable Energy Reviews, 81(1), 536–551.

[28] U.Alam, A.Khan, D. Ali, D.Bahnemann, M.Muneer (2018) Comparative photocatalytic activity of sol-gel derived rare earth metal (La, Nd, Sm and Dy)-doped ZnO photocatalysts for degradation of dyes, RSC Advances, 8, 17582–17594.

[29] X.Yang, H.Cai, M.Bao, J.Yu, J.Lu, Y.Li (2018) Insight into the highly efficient degradation of PAHs in water over graphene oxide/Ag_3PO_4 composites under visible light irradiation, Chemical Engineering Journal, 334, 355–376.

[30] Y.N. Xue, J.Y. Zhang, S. Tang, J.K. Liu, Y.B. Yue, X.H.Yang (2018) Rapid degradation of unmanageable polycyclic aromatic hydrocarbons by a C-ZnO solid solution nanocatalyst, New Journal of Chemistry, 42, 4308–4316.

[31] M.Farhadian, P. Sangpour, G. Hosseinzadeh (2016) Preparation and photocatalytic activity of WO_3–MWCNT nanocomposite for degradation of naphthalene under visible light irradiation, RSC Advances, 6(45), 39063–39073.

[32] J. Zhang, S. Fan, B. Lu, Q. Cai, J. Zhao, S. Zang (2019) Photodegradation of naphthalene over Fe_3O_4 under visible light irradiation, Royal Society Open Science, 6, 181779.

[33] A.D. Khatibi, K. Chandrika, F.K. Mostafapour, A.A. Sajadi, D. Balarak (2021) Photocatalytic Degradation of naphthalene By UV/ZnO: Kinetics, Influencing Factors and Mechanisms, Oriental Journal of Chemistry, 37(1), 65–70.

[34] A.D. Sekar, H. Muthukumar, N.I. Chandrasekaran, M. Matheswaran (2018) Photocatalytic degradation of naphthalene using calcined Fe-ZnO/PVA nanofibers, Chemosphere, 205, 610–617.

[35] H.Chen, M.Wen, Z.Huang, Q.Wu, J.Liu, T.Tu (2015) Construction of Cu@ZnO nanobrushes based on Cu nanowires and their high-performance selective degradation of polycyclic aromatic hydrocarbons, Journal of Materials Chemistry A, 3, 600–607.

IZVOD

FOTOKATALITIČKA DEGRADACIJA NAFTALENA, KORISTEĆI RAZLIČITE NANOKOMPOZITNE MATERIJALE, PRETEŽNO BAZIRANE NA OKSIDIMA METALA

Policiklični aromatični ugljovodonici (PAU) izazivaju značajnu zabrinutost u aspektima ekologije i zdravstva, što zahteva efikasne strategije njihovog uklanjanja. Na primer, biološki tretmani su efikasni samo za PAU jedinjenja nižih molekulskih masa, dok se za efikasno uklanjanje PAU složenijih struktura sve više preporučuje fotokatalitički metod. Fotokatalitička razgradnja se uglavnom oslanjala na materijale na bazi TiO$_2$. Međutim, ovaj revijalni rad fokusiran je na upotrebu različitih nanomaterijala za degradaciju, ili potpuno uklanjanje naftalena iz okoline, a posebno iz otpadnih voda. Preciznije rečeno, sagledana je fotokatalitička aktivnost različitih nanokompozitnih materijala koji (preovlađujuće) sadrže metalne okside, sa osvrtom na mehanizme fotokatalitičke razgradnje i identifikaciju međuprodukata. Ključni nalazi otkrivaju da ovi materijali imaju značajan potencijal i da fotogenerisane šupljine, superoksid radikali i hidroksil radikali igraju ključne uloge u procesima razgradnje naftalena, dodatno ističući jedinstvene mehanizme ovih procesa. Važne informacije o međuproduktima i putevima fotodegradacije iznete u diskusiji o mehanizmima razgradnje naftalena potvrđene su metodom gasne hromatografije sa masenom spektrometrijom (GC-MS).
Ključne reči: *Degradacioni mehanizmi, fotokataliza, naftalen, nanomaterijali*

Vladan Nedelkovski   https://orcid.org/0000-0001-7724-1118
Milan Radovanović   https://orcid.org/0000-0002-5175-6022
Slađana Alagić   https://orcid.org/0000-0002-2893-9285